DOI: http://dx.doi.org/10.32571/ijct.1272379 **E-ISSN: 2602-277X**

International Journal of Chemistry and Technology

http://dergipark.org.tr/ijct

Research Article

Investigation of the adsorption of dacarbazine (DTIC), which is used as an anticancer drug, on graphene oxide by DFT calculation method

Esvet AKBAŞ*, Begüm Cağla AKBAS

[1]*Department of Chemistry, Faculty of Science, Van Yuzuncu Yil University, 65080 Van-Türkiye*

[2]*Faculty of Pharmacy, University of Inonu, 44210, Malatya, Türkiye*

Received: 28 March 2023; Revised: 11 July 2023; Accepted: 8 September 2023

*****Corresponding author e-mail: esvakbas@hotmail.com

Citation: Akbas, B. C.; Akbas, E. *Int. J. Chem. Technol.* **2023**, 7 (2), 197-203.

ABSTRACT

Because of its superior properties, graphene oxide (GO) has become a potential candidate for nano-bio researchers to study its use in biomedical applications. Significant efforts have been made in recent years to explore the biomedical uses of graphene-based materials in smart medicine and genetic engineering. In this study, the electronic properties of commercially available dacarbazine (DTIC) used in cancer treatment and its adsorption on GO nanocage were calculated using density functional theory (DFT). DTIC is also known as imidazole carboxamide. It is an alkylating purine analogue chemotherapy drug used to treat melanoma and Hodgkin's lymphoma. Hodgkin usually uses it in combination with vinblastine, bleomycin, and doxorubicin. It is given by injection into a vein.

Keywords: Computational chemistry, organic molecule, nano-bio research, smart medicine.

1. INTRODUCTION

Graphene oxide, a single layer of graphene nanosheets functionalized with multiple oxygen-containing groups, was synthesized by oxidation of graphite to graphite oxide followed by exfoliation.[1] Graphene oxide contains a large number of epoxy and hydroxyl groups on its surface.[2-6] The carbon atom in the structure of graphene oxide makes sp^2 bonds and also provides resonance with an out-of-plane p orbital.[7] Graphene oxide has very good thermal, optical, electrical and magnetic properties. Due to these properties, it has an important place in materials science.[8, 9] Graphene oxide has a very large surface area. Due to this feature, it is a sought-after material in the fields of medicine, gene and tissue engineering.[10] In 2008, Liu et al. discovered the antineoplastic drug (*4S*)-4,11-diethyl-4,9-dihydroxy-1,4-dihydro- 3*H*, 14*H*-pyrano[3',4':6,7]indolizino. They demonstrated the adsorption of [1,2-b]quinoline-3,14-dione (SN38) on graphene in biological systems[11,12] (Figure 1). After this development, research with graphene-derived materials for the development of drug delivery systems increased exponentially.

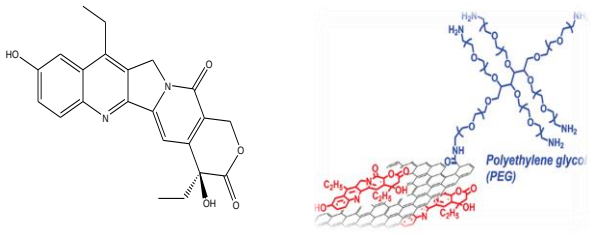

Figure 1. SN38 and NGO−PEG−SN38 complex. [11]

In this study, the interaction of the chemotherapeutic drug dacarbazine "(5-(3,3-dimethyl-1-triazenyl)imidazole-4-carboxamide)" (DTIC) [13] (Figure 2) with graphene oxide was calculated using density functional theory (DFT). DTIC is a purine analog drug active ingredient containing imidazole carboxamide derivative used in cancer treatment. It is mostly used in the treatment of lymphoma.

DOI: http://dx.doi.org/10.32571/ijct.1272379 E-ISSN: 2602-277X

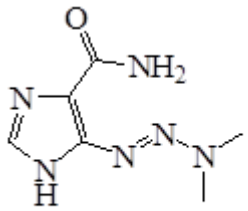

Figure 2. DTIC.

The purpose of this work is to calculation of the drug/ graphene oxide (GO) nanocage system for controlled DTIC recognition. Calculations and analyzes are performed on values such as molecular electronic properties and adsorption energy of the system. In addition, the nature of the interactions is facilitated through the use of features such as nonlinear optics (NLO).

2. MATERIALS AND METHODS

The adsorption of DTIC on the GO nanocage surface was investigated by DFT calculations. The calculations are made on Gaussian09 program *using* the B3LYP/6-31 G (d, p) basis set.[14] This basis set is very useful for nanostructural frameworks. [15, 16] To accurately predict the weak interaction, the adsorption energies (ΔEad) were calculated as follows:

$$\Delta Ead = \Delta E(complex) - \Delta E(GO) - \Delta E(drug) \quad 1)$$

Quantum chemical parameters ΔE_{HOMO}, ΔE_{LUMO} and ΔE_{gap} were calculated and discussed for all types of interactions.

In addition, electronegativity "χ", chemical softness "S", ionization potential "I", dipole moment "μ", chemical hardness "η" and electron affinity "A" [17,18] calculations were performed for GO and DTIC.

2. RESULT AND DISCUSSION

Full geometry optimizations of the GO nanocage, DTIC and all interactions were performed using DFT based on Beck and Lee–Yang–Parr [19] non-local correlation functional (B3LYP) 6-31G (d, p) basis sets in the Gaussian09 program [14] (Fig. 3).

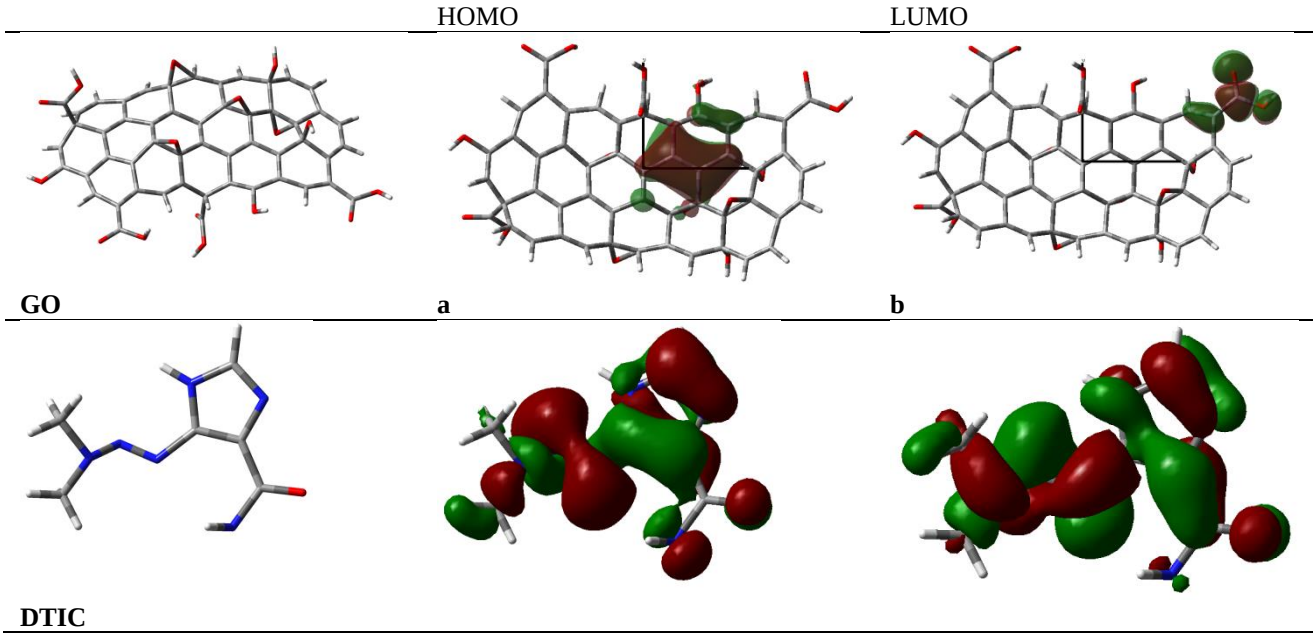

Figure. 3. Optimized structures of GO nanocage, DTIC, all interactions and their HOMO and LUMO profile.

The HOMO of the GO nanocage is mainly localized at the epoxy group sites (**a**) and the LUMO located at the carboxylic acid sites (**b**). The LUMO level of the GO is mainly due to the "C-C" bond and the HOMO is mainly due to the "O" atoms.

The adsorption activity of DTIC on GO can be analyzed by theoretical calculations. HOMO and LUMO values obtained by theoretical calculations are the most important parameters used to predict the adsorption activity of DTIC on the GO surface. In addition, parameters such as ionization potential, electron affinity,
chemical softness, dipole moment, chemical hardness and electronegativity can be obtained by quantum calculations (Table 1).

Koopman [20] has equated the relationship of the E_{HOMO} and E_{LUMO} of the compound with the ionization potential (I) and electron affinity (A). Accordingly,

DOI: http://dx.doi.org/10.32571/ijct.1272379 **E-ISSN: 2602-277X**

electron affinity and ionization potential can be defined as I = - E_{HOMO} and A = - E_{LUMO}. Adhering to these calculations, the absolute electronegativity (χ) and chemical hardness (η) of the compound can be written as follows; [21]

$$\chi = -\mu = \left(\frac{-E_{HOMO}-E_{LUMO}}{2}\right) = \left(\frac{I+A}{2}\right) \quad (2)$$

$$\eta = \frac{1}{2}\left(\frac{\partial^2 E}{\partial N^2}\right)_{\vartheta(r)} = \frac{1}{2}\left(\frac{\partial \mu}{\partial N}\right) \quad (3)$$

In calculations, chemical hardness (η) and softness (S) are also important parameters that show the reactivity for compounds. These values depend on each other as in the equation below.

$$S = \frac{1}{\eta} \quad (4)$$

Table 1. The quantum chemical parameters for GO and DTIC (eV).

Structure	E_{HOMO}	E_{LUMO}	ΔE	I	A	η	S	χ	μ
GO	-7.1693	-0.9750	6.1943	7.1693	0.9750	6.1943	0.1614	4.0722	6.4721
DTIC	- 5.8165	- 3.1938	2.6227	5.8165	3.1938	2.6227	0.3813	4.0722	8.9948

Nonlinear optical properties of GO and DTIC compounds were calculated using the B3LYP/6-31+G (d, p) base set in the gas phase. As a result of these calculations, total dipole moment μ_{tot}, average polarizability (α_{tot}) and average first hyperpolarizability (β_{tot}) were calculated for the compounds.

$$\mu tot = \mu_X^2 + \mu_Y^2 + \mu_Z^2 \quad (5)$$

$$\alpha tot = (\alpha_{xx} + \alpha_{yy} + \alpha_{zz})/3 \quad (6)$$

$$\beta tot = [(\beta_{xxx} + \beta_{xyy} + \beta_{xzz})^2 + (\beta_{yxx} + \beta_{yxx} + \beta_{yzz})^2 + (\beta_{zzz} + \beta_{zxx} + \beta_{zyy})^2]^{\frac{1}{2}} \quad (7)$$

The values obtained as a result of the calculations are given in Table 2. High dipole moment, molecular polarizability and hyperpolarizability values indicate that the compound has good non-linear optical (NLO) properties. According to the values obtained as a result of the calculations for GO and DTIC molecules, these compounds have very good NLO properties.

Table 2. μ, α and β for GO and DTIC.

Parameters (a.u)	GO	DTIC
β_{xxx}	589.8926	-147.7707
β_{xyy}	155.7559	-21.1920
β_{xzz}	-60.7116	1.8824
β_{yyy}	-269.3956	53.6089
β_{yxx}	-228.1507	14.7872
β_{yzz}	78.0111	-7.8043
β_{zzz}	-51.6876	0.1728
β_{xxz}	69.4933	-3.4920
β_{zyy}	7.4148	-5.0818
β_{tot} (esu) 10^{-33}	803.607	177.9263
α_{xx}	17.9609	-12.4096
α_{yy}	-1.5240	9.8781
α_{zz}	-16.4370	2.5315
α_{tot} (esu) 10^{-33}	-0.00003	0
μ_x	4.3060	-8.1204
μ_y	-4.6709	3.7396
μ_z	1.2362	-0.9890
μ_{tot} (esu) 10^{-33}	6.4720	8.9946

The molecular electrostatic potential maps (MEPs) were calculated using DFT and B3LYP (d, p) base set in the Gaussian09 program for GO and DTIC molecules. In MEPs, which provide important information about the charge distribution of the molecules, the charge distributions are given in different colours. In the MEPs given in Figure 4, the areas represented in red represent the regions where negativity is concentrated in the molecule (nucleophile), and the regions in blue color represent the areas in the molecule where positivity is concentrated (electrophile). The electrostatic potential increases during red> orange> yellow> green> blue. In these our compounds the highest potential is on oxygen atoms. As shown in Figure 4, seven different DTIC heads are capable of attacking the nanocage. The various initial DTIC/GO structures (designated I, II, III and IV), as shown in Figure 5, have been optimized. Interactions are reported as Angstrom (A^o) values.

DOI: http://dx.doi.org/10.32571/ijct.1272379 E-ISSN: 2602-277X

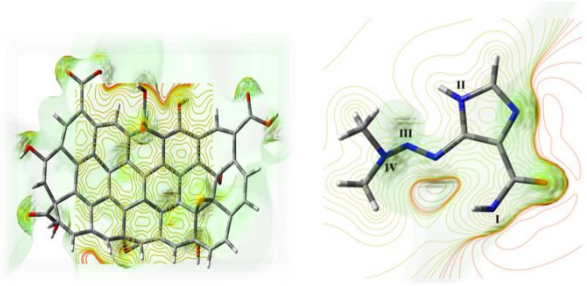

GO **DTIC**

Fig. 4. MEPs for GO and DTIC molecules.

The calculation of the binding properties of the DTIC/GO complexes was carried out in different states, as shown in Figure 5. Consequently, complex **2** is the most stable due to the interaction between DTIC and the GO nanocage from its NH_2 group side (1.43).

Calculation of the energies of the DTIC/GO complexes showed that the electronic energy for complex **2** was approximately -104372 (*eV*) (Table 3).

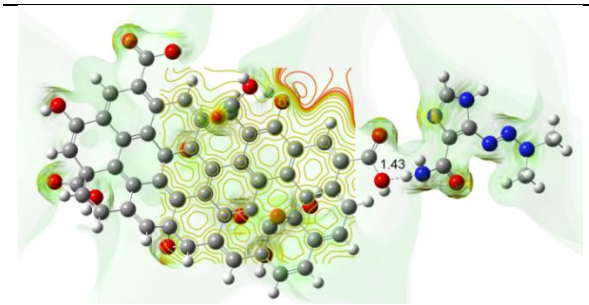

1

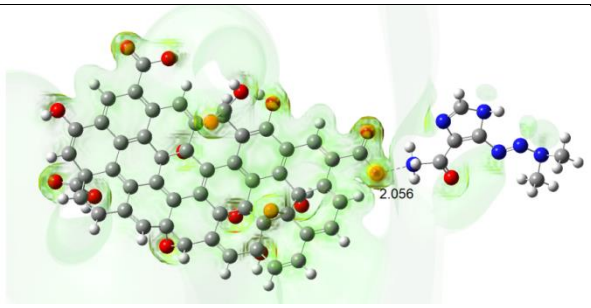

2

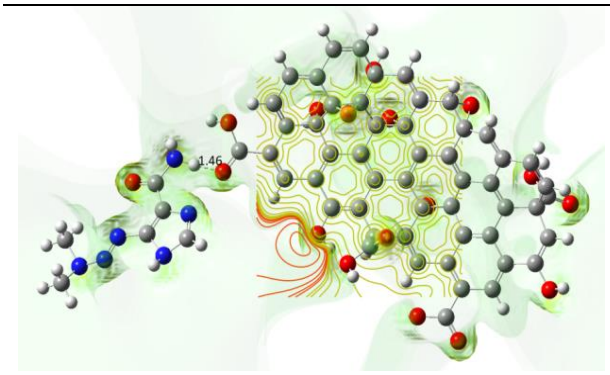

3

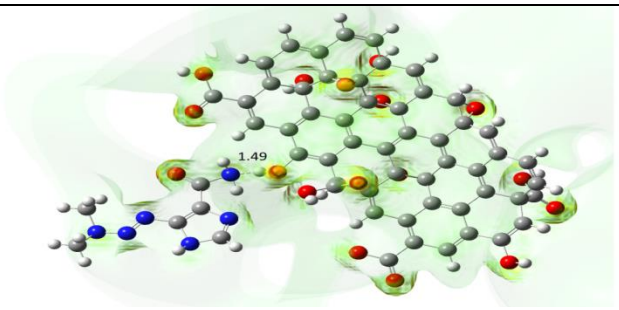

4

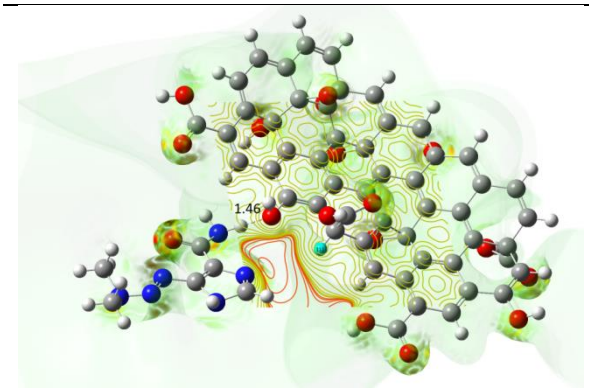

5

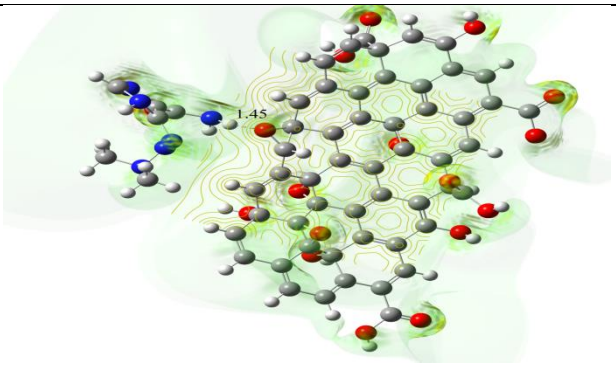

6

DOI: http://dx.doi.org/10.32571/ijct.1272379 E-ISSN: 2602-277X

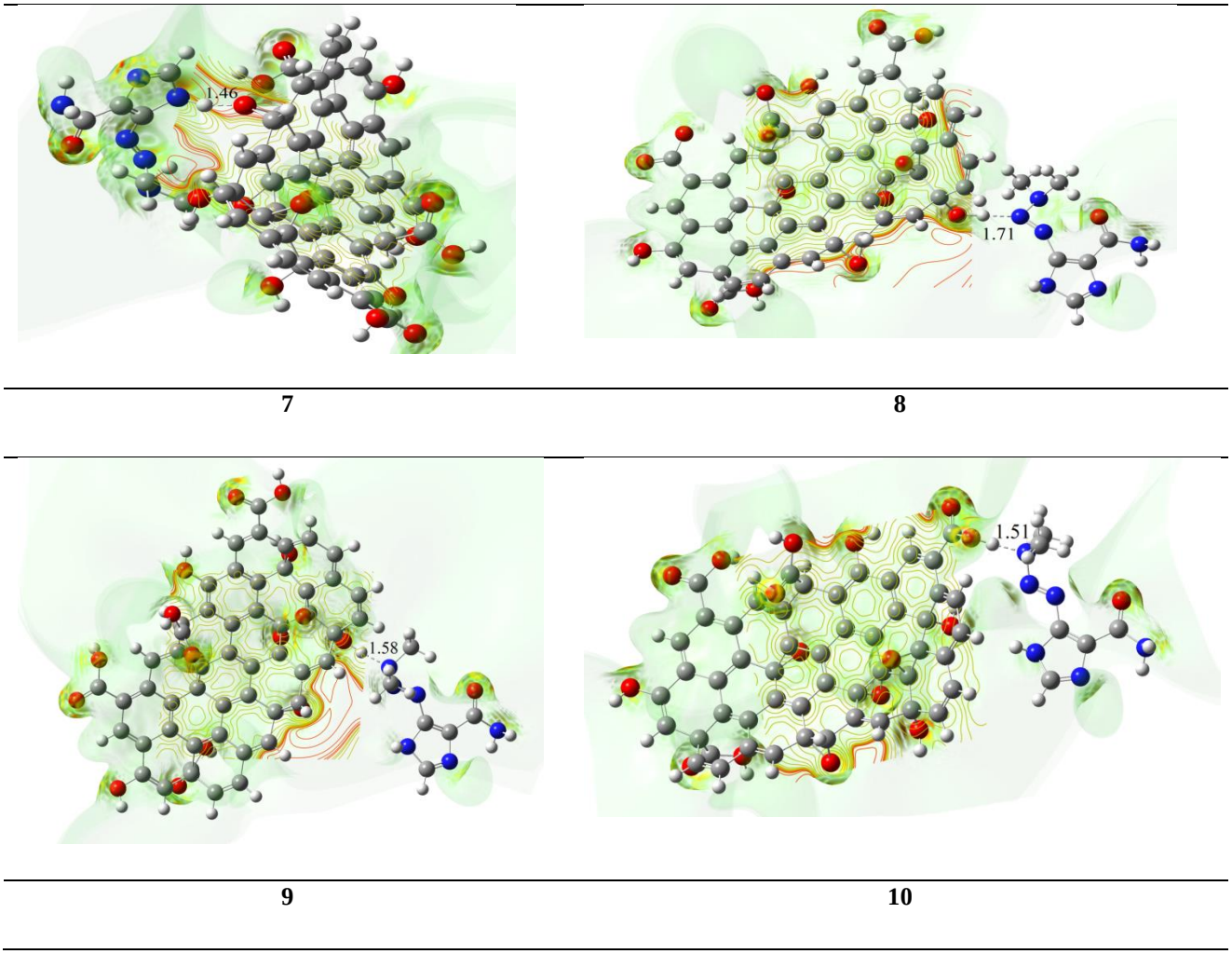

7 **8**

9 **10**

Figure 5. DTIC/GO complexes.

Table 3. Calculated were electronic energies for complexes.

Complexes	$\Delta E_{(complex)}$ (eV)	ΔE_{ad} (eV)
1	-104380	-192550
2	-104372	-192542
3	-104381	-192551
4	-104381	-192551
5	-104382	-192552
6	-104374	-192544
7	-104382	-192552
8	-104376	-192546
9	-104380	-192550
10	-104384	-192554

When the adsorption energies are compared, it is seen that **2** has a higher adsorption energy value. Accordingly, the two main mechanisms involved in the adsorption of DTIC to the carboxylic acid site on the GO nanokage surface are orbital and charge-induced interactions (electrostatic effect). In particular, the hydrogen atom bonded to the nitrogen atom interacts with the oxygen in the carboxylic acid group, inducing intermolecular electrostatic interactions. Consequently, complex **2** is the most stable from its NH_2 side due to the interaction between DTIC and the GO nanocage.

Figure 6 shows the density of the state spectra for DTIC and complex **2**. The decrease in the Eg value of the GO-DTIC compared to the GO nanocage is due to this opposite electric peak after the adsorption process of DTIC. Furthermore, a closer examination of the DOS spectrum reveals that the HOMO and especially the

DOI: http://dx.doi.org/10.32571/ijct.1272379 **E-ISSN: 2602-277X**

LUMO levels are shifted to the higher energy region after adsorption of DTIC.

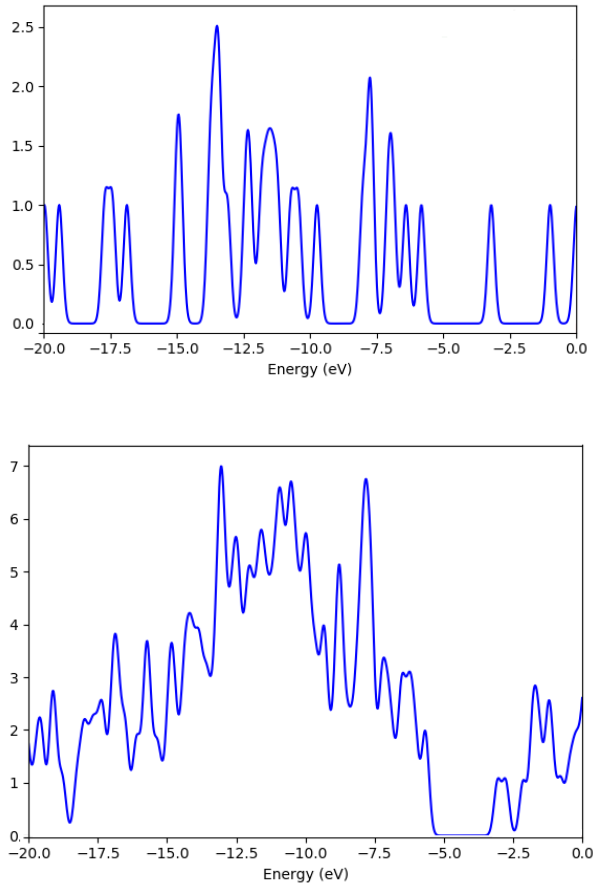

Figure 6. DOS plots of pristine DTIC drug and complex 2.

3. CONCLUSIONS

The adsorption value between DTIC and GO nanocage was evaluated using quantum chemical calculations to create a new drug detection system. As a result of the calculations, it was observed that the adsorption occurred as a result of the interaction of the COOH groups on the GO nanolattice surface and the $CONH_2$ group in the drug. When the obtained data are interpreted, it has been determined that the molecular electrostatic interactions of the groups are also effective on the adsorption occurring on the surface.

Conflict of interests

I declare that there is no a conflict of interest with any person, institute, company, etc.

REFERENCES

1. Krishnamoorthy K.; Kim G.S.; Kim S.J. *Ultrason, Sonochem*. **2013**, 20, 644–649.

2. Mouhat F.; Coudert F. X.; Bocquet L. M. *Nature Communications*, **2020**, 11(1)1566.

3. Valentini L.; Bittolo Bon S.; Giorgi G. *Polymers (Basel)*, **2020**, 12(7) 1596.

4. Ramesha G.K.; Kumara A.V.; Muralidhara H.B.; Sampath S. *J.Colloid Interface Sci.* **2011,** 361 270–277.

5. Zhu J.; Wei S.; Gu H.; Rapole S.B.; Wang Q.; Luo Z.; Haldolaarachchige N.; Young D.P.; Guo Z. *Environ. Sci. Technol.* **2012,** 46 (2) 977–985.

6. Tiwari J.N.; Mahesh K.; Le N.H.; Timilsina K.C.K.R.; Tiwari R.N.; Kim K.S. *Carbon*, **2013,** 56 173–182.

7. Bai J.; Zhong X.; Jiang S.; Huang Y.; Duan X. *Nat Mater.*, **2010,** 5 190–194.

8. Li Z.; Fan J.; Tong C.; et al. *Nanomedicine*, **2019,** 14(15) 2011–2025.

9. Fedotova A. K.; Prischepa S. L.; Fedotova J.; et al., *Physica E: Low-dimensional Systems and Nanostructures*, **2020,** 117 113790.

10. Jiang J.H.; Pi J.; Jin H.; Cai J. Y. *Arti Cells Nanomed Biotechnol*, **2018,** 46(3) 297–307.

11. Liu Z.; Robinson J.T.; Sun X.; Dai H. *J. Am. Chem. Soc.*, **2008,** 130(33) 10876–10877.

12. Hoseini-Ghahfarokhi M.; Mirkiani S.; Mozaffari N.; Abdolahi Sadatlu M.A.; Ghasemi A.; Abbaspour S.; Akbarian M.; Farjadian F.; Karimi M. *International Journal of Nanomedicine*, **2020,** 15 9469–9496.

13. Elks J.; Ganellin C. R. *The Dictionary of Drugs*, **1990,** 344.

14. Gaussian 09, Revision D.01, Frisch M. J.; Trucks G. W.; Schlegel H. B.; Scuseria G. E.; Robb M. A.; Cheeseman J. R.; Scalmani G.; Barone V.; Mennucci B.; Petersson G. A.; H Nakatsuji.; Caricato M.; Li X.; Hratchian H. P.; Izmaylov A. F.; Bloino J.; Zheng G.; Sonnenberg J. L.; Hada M.; Ehara M.; Toyota K.; Fukuda R.; Hasegawa J.; Ishida M.; Nakajima T.; Honda Y.; Kitao O.; Nakai H.; Vreven T.; Montgomery J. A.; Peralta Jr. J. E.; Ogliaro F.; Bearpark M.; Heyd J. J.; Brothers E.; Kudin K. N.; Staroverov V. N.; Kobayashi R.; Normand J.; Raghavachari K.; Rendell A.; Burant J. C.; Iyengar S. S.; Tomasi J.; Cossi M.; Rega N.; Millam J. M.; Klene M.; Knox J. E.; Cross J. B.; Bakken V.; Adamo C.; Jaramillo J.; Gomperts R.; Stratmann R. E.; Yazyev O.; Austin A. J.; Cammi R.; Pomelli C.; Ochterski J. W.; Martin R. L.; Morokuma K.; Zakrzewski V. G.; Voth G. A.; Salvador P.; Dannenberg J. J.; Dapprich S.; Daniels A. D.; Farkas Ö.; Foresman J. B.; Ortiz J. V.; Cioslowski J. and Fox D. J. *Gaussian, Inc., Wallingford, CT, USA*, (**2009**).

15. Perdew J. P.; Wang Y. *Phys. Rev. B. Condens. Matter*; **1992,** 45 13244–13249.

DOI: http://dx.doi.org/10.32571/ijct.1272379 **E-ISSN: 2602-277X**

16. Simos T. E.; Tsitouras C.; Kovalnogov V. N.; Fedorov R. V.; Generalov D. A. *Mathematics (Basel)*, **2021,** 9 664.

17. Karzazi Y.; Belghiti M.E. A.; Dafali A.; and Hammouti B. *Journal of Chemical and Pharmaceutical Research*, **2014,** 6(4) 689-696.

18. Glendening E. D.; Landis C. R.; Weinhold F. *Program. J. Comput. Chem*. **2013,** 341429–1437.

19. Lee C.; Yang W.; Parr R. G. *Phys. Rev. B.* **1988,** 37, 785.

20. Wang H.; Wang X.; Wang H.; Wang L.; Liu A. *J. Mol. Model.*, **2007,** 13 147.

21. Fleming I.; Frontier Orbitals and Organic Chemical Reactions, John Wiley and Sons, NewYork,. (**1976**).